

# Muon Anomalous Magnetic Moment and Gauge Symmetry in the Standard Model

Er-Cheng Tsai\*

*Physics Department, National Taiwan University, Taipei, Taiwan*

## Abstract

No gauge invariant regularization is available for the perturbative calculation of the standard model. One has to add finite counter terms to restore gauge symmetry for the renormalized amplitudes. The muon anomalous magnetic moment can be accurately measured but the experimental result does not entirely agree with the theoretical calculation from the standard model. This paper is to compute the contributions to the muon gyromagnetic ratio  $g_\mu$  due to the finite counter terms. The result obtained is found to be far from sufficient to explain the discrepancy between theory and experiment.

PACS numbers: 11.10.Gh, 11.15.Bt, 12.15.Lk, 13.40.Em, 14.60.Ef

Keywords: magnetic moment; muon;  $\gamma_5$ ; dimensional regularization; chiral fermion; renormalization; electroweak

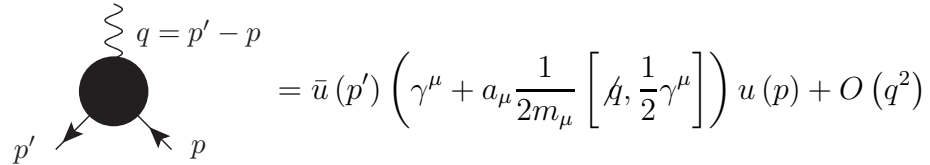
---

\* ectsai@ntu.edu.tw

## I. INTRODUCTION

The magnetic moment of a muon is  $\vec{M} = g_\mu \frac{e}{2m_\mu} \vec{S}$  where the gyromagnetic ratio  $g_\mu$  is equal to 2 if quantum loop corrections are ignored.  $g_\mu$  can be measured quite precisely and its derivation from the classical value is found to be  $\frac{g_\mu - 2}{2} = 11659209.1 \times 10^{-10}$  [1, 2]. Within the framework of the standard model,  $\frac{g_\mu - 2}{2}$  can be calculated and its theoretical value compared to the experimental result therefore offers a precise test of the standard model at quantum loop level.

The electromagnetic form factors can be written as:



$$= \bar{u}(p') \left( \gamma^\mu + a_\mu \frac{1}{2m_\mu} \left[ \not{q}, \frac{1}{2} \gamma^\mu \right] \right) u(p) + O(q^2)$$

with  $p^2 = p'^2 = m_\mu^2$  and  $a_\mu = \frac{g_\mu - 2}{2}$  [3]. In the standard model higher order corrections of  $a_\mu$  are classified into QED, electroweak (EW) and hadronic classes:

$$a_\mu = a_\mu^{QED} + a_\mu^{EW} + a_\mu^{Had}$$

The QED part is known to 4-loops and leading terms in 5-loops [4].

$$\begin{aligned} a_\mu^{QED} &= \left(\frac{\alpha}{\pi}\right) 0.5 + \left(\frac{\alpha}{\pi}\right)^2 0.765857410(27) + \left(\frac{\alpha}{\pi}\right)^3 24.05050964(87) \\ &+ \left(\frac{\alpha}{\pi}\right)^4 130.8055(80) + \left(\frac{\alpha}{\pi}\right)^5 663(20) \\ &= 116584718.09(0.15) \times 10^{-11} \end{aligned} \quad (1)$$

The electroweak part  $a_\mu^{EW}$  is the loop contribution due to heavy  $W^\pm$ ,  $Z$  or Higgs particle and is suppressed by at least a factor of

$$\frac{\alpha}{\pi} \frac{m_\mu^2}{m_W^2} \simeq 4 \times 10^{-9},$$

which enables us to neglect the 3-loop terms. The 1-loop [5]

$$a_\mu^{EW} [1\text{-loop}] = 194.8 \times 10^{-11}$$

and leading term in 2-loop [6]

$$a_\mu^{EW} [2\text{-loop}] = -40.7 \times 10^{-11}$$

add up to give the total

$$a_{\mu}^{EW} = 154 \times 10^{-11}. \quad (2)$$

The hadronic part is evaluated via dispersion relation approach, the available  $\sigma(e^+e^- \rightarrow \text{hadrons})$  data give rise [7] to a leading-order hadronic vacuum polarization contribution of [8]

$$a_{\mu}^{Had} [LO] = 6923 (42) (3) \times 10^{-11}. \quad (3)$$

Higher order hadronic contribution is found to be [9]

$$a_{\mu}^{Had} [NLO] = 7 (26) \times 10^{-11} \quad (4)$$

Adding (1), (2), (3) and (4) gives the standard model prediction based on  $e^+e^-$  data.

$$a_{\mu}^{SM} = 116591803 (1) (42) \times 10^{-11}$$

The difference between experiment and theory is

$$\Delta a_{\mu} = a_{\mu}^{\text{exp}} - a_{\mu}^{SM} = 281 (63) (49) \times 10^{-11} \quad (5)$$

New physics effects beyond standard model have been pondered over to explain this discrepancy.

The dimensional regularization scheme proposed by 't Hooft and Veltman [10] is a very convenient scheme for regularizing gauge theory without  $\gamma_5$ , such as QED. For chiral gauge theories involving  $\gamma_5$ , no gauge invariant regularization is available but the dimensional regularization can still be used in a rigorous manner by maintaining

$$\gamma_5 = i\gamma^0\gamma^1\gamma^2\gamma^3 \quad (6)$$

even when the space-time dimension  $n$  departs from 4 [11]. Such  $\gamma_5$  anticommutes with  $\gamma^{\mu}$  for  $\mu$  in the first 4 dimensions but commutes with  $\gamma^{\mu}$  when the index  $\mu$  goes beyond the first 4 dimensions. The continuation to  $n \neq 4$  for the Lagrangian of a theory with a gauge invariant 4 dimensional Lagrangian depends on how we express and continue the terms involving  $\gamma_5$  in the Lagrangian. The breakdown of gauge symmetry in this scheme can be remedied by introducing additional finite gauge variant local counter terms to restore the gauge symmetry [12]. One ingredient that was missing in the previous evaluation of the electroweak part  $a_{\mu}^{EW}$  is the contribution due to these finite counter terms that must be invoked to restore gauge symmetry. In this paper, we will calculate the correction to the muon gyromagnetic ratio due to the lowest order finite counter terms. It turns out that the result obtained is not significant enough to account for the difference (5).

## II. STANDARD MODEL

The gauge group for the standard model is  $SU(3) \times SU(2) \times U(1)$  with three kinds of vector gauge bosons,  $G^{\mu,a}$ ,  $a = 1, 2, \dots, 8$  for  $SU(3)$ ,  $W^{\mu,a}$ ,  $a = 1, 2, 3$  for  $SU(2)$ , and  $B^\mu$  for  $U(1)$ . Let  $S^a$ ,  $a = 1, 2, \dots, 8$  and  $T^a$ ,  $a = 1, 2, 3$  be the traceless, Hermitian generators for  $SU(3)$  and  $SU(2)$  in the adjoint representation. They are normalized as

$$\text{Tr}(S^a S^b) = \frac{1}{2} \delta^{ab}, \text{Tr}(T^a T^b) = \frac{1}{2} \delta^{ab} \quad (7)$$

with the commutators

$$[S^a, S^b] = i f^{abc} S^c, [T^a, T^b] = i \epsilon^{abc} T^c$$

We choose  $T^a = \frac{\sigma_a}{2}$  as the  $SU(2)$  generator with  $\sigma_a$  being the Pauli matrix. Define the matrix fields

$$G^\mu = \sum_{a=1}^8 G_a^\mu S^a, W^\mu = \sum_{a=1}^3 W_a^\mu T^a$$

and the covariant derivatives

$$D_S^\mu = \partial^\mu + i g_S G^\mu, D_W^\mu = \partial^\mu + i g_W W^\mu, D_B^\mu = \partial^\mu + i \frac{g_B}{2} B^\mu,$$

for  $SU(3)$ ,  $SU(2)$  and  $U(1)$  with coupling constants  $g_S$ ,  $g_W$  and  $g_B$  respectively. Let

$$G^{\mu\nu} = \frac{1}{i g_S} [D_S^\mu, D_S^\nu] = \partial^\mu G^\nu - \partial^\nu G^\mu + i g_S [G^\mu, G^\nu],$$

$$W^{\mu\nu} = \frac{1}{i g_W} [D_W^\mu, D_W^\nu] = \partial^\mu W^\nu - \partial^\nu W^\mu + i g_W [W^\mu, W^\nu],$$

and

$$B^{\mu\nu} = \partial^\mu B^\nu - \partial^\nu B^\mu.$$

The Lagrangian for the standard model without matter fields is

$$\begin{aligned} L_1 = & -\frac{1}{2} \text{Tr}(G_{\mu\nu} G^{\mu\nu}) - \frac{1}{2} \text{Tr}(W_{\mu\nu} W^{\mu\nu}) - \frac{1}{4} B_{\mu\nu} B^{\mu\nu} \\ & + (D_H^\mu \phi)^\dagger (D_{H\mu} \phi) - \frac{\lambda}{8} g^2 \left( \phi^\dagger \phi - \frac{v^2}{2} \right)^2 \end{aligned} \quad (8)$$

where the Higgs  $\phi$  is a two component scalar complex field coupled to  $W$  and  $B$  gauge bosons with

$$D_H^\mu \phi = \left( \partial^\mu + i g_W W^\mu - i \frac{g_B}{2} B^\mu \right) \phi$$

$\phi$  is assumed to have the vacuum expectation value:

$$\langle \phi \rangle = \frac{1}{\sqrt{2}} \begin{bmatrix} 0 \\ v \end{bmatrix}$$

Express  $\phi$  in terms of four real components  $H$  and  $\phi_a$ ,  $a = 1, 2, 3$ :

$$\begin{aligned} \phi &= \frac{1}{\sqrt{2}} \begin{bmatrix} i\phi_1 + \phi_2 \\ H + v - i\phi_3 \end{bmatrix} = \frac{1}{\sqrt{2}} \begin{bmatrix} H + v + i\phi_3 & i\phi_1 + \phi_2 \\ i\phi_1 - \phi_2 & H + v - i\phi_3 \end{bmatrix} \begin{bmatrix} 0 \\ 1 \end{bmatrix} \\ &= \frac{1}{\sqrt{2}} (H + v + i\phi_a \sigma^a) \begin{bmatrix} 0 \\ 1 \end{bmatrix} = \hat{\phi} \begin{bmatrix} 0 \\ 1 \end{bmatrix} \end{aligned} \quad (9)$$

where  $\hat{\phi}$  is defined as

$$\hat{\phi} = \frac{1}{\sqrt{2}} (H + v + i\phi_a \sigma^a).$$

Note that

$$\hat{\phi} \begin{bmatrix} 1 \\ 0 \end{bmatrix} = \frac{1}{\sqrt{2}} \begin{bmatrix} H + v + i\phi_3 \\ i\phi_1 - \phi_2 \end{bmatrix} = i\sigma_2 \left( \frac{1}{\sqrt{2}} \begin{bmatrix} i\phi_1 + \phi_2 \\ H + v - i\phi_3 \end{bmatrix} \right)^* = i\sigma_2 \hat{\phi}^* \begin{bmatrix} 0 \\ 1 \end{bmatrix}$$

Under a  $SU(2) \times U(1)$  transformation

$$\phi = \hat{\phi} \begin{bmatrix} 0 \\ 1 \end{bmatrix} \rightarrow e^{-ig_W \theta_a T_a} e^{i\frac{g_B}{2} \chi} \hat{\phi} \begin{bmatrix} 0 \\ 1 \end{bmatrix} \quad (10)$$

and, since  $(i\sigma_2) \vec{\sigma}^* = -\vec{\sigma} (i\sigma_2)$ ,

$$\hat{\phi} \begin{bmatrix} 1 \\ 0 \end{bmatrix} \rightarrow i\sigma_2 e^{ig_W \theta_a T_a^*} e^{-i\frac{g_B}{2} \chi} \hat{\phi}^* \begin{bmatrix} 0 \\ 1 \end{bmatrix} = e^{-ig_W \theta_a T_a} e^{-i\frac{g_B}{2} \chi} \hat{\phi} \begin{bmatrix} 1 \\ 0 \end{bmatrix} \quad (11)$$

Replacing  $\phi$  by  $\frac{1}{\sqrt{2}} \begin{bmatrix} 0 \\ v \end{bmatrix}$  in  $(D_H^\mu \phi)^\dagger (D_{H\mu} \phi)$ , we obtain the following quadratic mass term for the vector bosons.

$$\begin{aligned} &\frac{v^2}{2} \begin{bmatrix} 0 & 1 \end{bmatrix} \left( g_W W^\mu - \frac{g_B}{2} B^\mu \right)^2 \begin{bmatrix} 0 \\ 1 \end{bmatrix} \\ &= \frac{v^2}{2} \left( \left( \frac{g_W}{2} \right)^2 \left( (W_1^\mu)^2 + (W_2^\mu)^2 \right) + \left( \frac{g_W}{2} W_3^\mu + \frac{g_B}{2} B^\mu \right)^2 \right) \end{aligned}$$

Define

$$\begin{bmatrix} A^\mu \\ Z^\mu \end{bmatrix} = \frac{1}{\sqrt{g_W^2 + g_B^2}} \begin{bmatrix} g_W & -g_B \\ g_B & g_W \end{bmatrix} \begin{bmatrix} B^\mu \\ W^\mu \end{bmatrix}. \quad (12)$$

The vector field  $A^\mu$  is massless and is identified as the photon field.

The Lagrangian (8) is invariant under the following BRST [13] variations with Grassmann ghost fields  $c_S = \sum_{a=1}^8 c_S^a S^a$ ,  $c_W = \sum_{a=1}^3 c_W^a T^a$ ,  $c_B$  as the parameters for the  $SU(3)$ ,  $SU(2)$ ,  $U(1)$  groups.

$$\begin{aligned}\delta G^\mu &= [D_S^\mu, c_S], \delta W^\mu = [D_W^\mu, c_W], \delta B_\mu = \partial_\mu c_B, \\ \delta\phi &= -i \left( g_W c_W - \frac{g_B}{2} c_B \right) \phi\end{aligned}\tag{13}$$

The gauge fixing and corresponding ghost terms [14] in the pure alpha gauge are

$$\begin{aligned}L_{gf} &= -\frac{1}{\alpha_S} \text{Tr} (\partial_\mu G^\mu)^2 - \frac{1}{\alpha_W} \text{Tr} (\partial_\mu W^\mu)^2 - \frac{1}{2\alpha_B} (\partial_\mu B^\mu)^2 \\ &\quad + 2\text{Tr} (i\bar{c}_S \delta (\partial_\mu G^\mu)) + 2\text{Tr} (i\bar{c}_W \delta (\partial_\mu W^\mu)) + i\bar{c}_B \delta (\partial_\mu B^\mu)\end{aligned}\tag{14}$$

where  $\bar{c}_S$ ,  $\bar{c}_W$ ,  $\bar{c}_B$  are the anti-ghosts corresponding to  $c_S$ ,  $c_W$ ,  $c_B$  and the BRST variations for ghost and anti-ghost fields are

$$\begin{aligned}\delta c_S^a &= \frac{g_S}{2} f^{abc} c_S^b c_S^c, \delta c_W^a = \frac{g_W}{2} \epsilon^{abc} c_W^b c_W^c, \delta c_B = 0, \\ \delta \bar{c}_S &= -\frac{i}{\alpha_S} \partial_\mu G^\mu, \delta \bar{c}_W = -\frac{i}{\alpha_W} \partial_\mu W^\mu, \delta \bar{c}_B = -\frac{i}{\alpha_B} \partial_\mu B^\mu.\end{aligned}$$

There are three generations of fermion matter fields consisting of quarks

$$\begin{pmatrix} u \\ d \end{pmatrix}, \begin{pmatrix} c \\ s \end{pmatrix}, \begin{pmatrix} t \\ b \end{pmatrix}$$

and leptons

$$\begin{pmatrix} \nu_e \\ e \end{pmatrix}, \begin{pmatrix} \nu_\mu \\ \mu \end{pmatrix}, \begin{pmatrix} \nu_\tau \\ \tau \end{pmatrix}\tag{15}$$

Note for simplicity, we have suppressed the color indices of quarks. We will use the notation  $\psi_i = \begin{pmatrix} \psi_i^u \\ \psi_i^d \end{pmatrix}$  indexed by  $i$  to denote the above fermion fields. The  $G^\mu$  gluons couple only to the quark fields with equal strength for left-handed and right-handed quarks.  $W$  and  $B$  gauge bosons couple to both left-handed quarks and left-handed leptons. The chiral projection operators  $L$  and  $R$  are defined as

$$L = \frac{1}{2} (1 - \gamma_5), R = \frac{1}{2} (1 + \gamma_5).$$

The right-handed fermion  $\psi_R = R\psi$  is a  $SU(2)$  singlet and thus is not coupled to  $W$ . The covariant derivative for a left-handed quark  $\psi_L = L\psi$  is

$$D_{q,L}^\mu L\psi_i = \left( \partial^\mu + ig_S G^\mu + ig_W W^\mu - iY_i \frac{g_B}{2} B^\mu \right) L\psi_i \quad (16)$$

and that for a left-handed lepton is

$$D_{l,L}^\mu L\psi_i = \left( \partial^\mu + ig_W W^\mu - iY_i \frac{g_B}{2} B^\mu \right) L\psi_i \quad (17)$$

where  $Y_i$  is the weak hypercharge. Using the inverse of (12) to express  $(B, W)$  in terms of  $(A, Z)$ , we get

$$\begin{aligned} g_W W_3^\mu T^3 - \frac{g_B}{2} Y_i B^\mu &= \left( \frac{g_W}{2} W_3^\mu + \frac{g_B}{2} B^\mu \right) \sigma_3 - (Y_i + \sigma_3) \frac{g_B}{2} B^\mu \\ &= -\frac{(Y_i + \sigma_3)}{2} \frac{g_B g_W}{\sqrt{g_W^2 + g_B^2}} A^\mu \\ &\quad + \frac{g_W^2 \sigma_3 - Y_i g_B^2}{2\sqrt{g_W^2 + g_B^2}} Z^\mu, \end{aligned}$$

The electric charge for the left-handed fermion is proportional to  $\frac{(Y_i + \sigma_3)}{2} g_B$ . The weak hypercharge for the right-handed fermions must also be  $\frac{(Y_i + \sigma_3)}{2} g_B$  so that the electric charges for the left-handed and right-handed fermions may be the same. The covariant derivative for a right-handed quark is

$$D_{q,R}^\mu R\psi_i = \left( \partial^\mu + ig_S G^\mu - i \frac{(Y_i + \sigma_3)}{2} g_B B^\mu \right) R\psi_i \quad (18)$$

and that for a right-handed lepton is

$$D_{l,R}^\mu R\psi_i = \left( \partial^\mu - i \frac{(Y_i + \sigma_3)}{2} g_B B^\mu \right) R\psi_i. \quad (19)$$

It is known that  $Y_i = -1$  for all leptons and  $Y_i = \frac{1}{3}$  for all quarks.

The transformations (10) and (11) for  $\hat{\phi}$  can be utilized to show that the following four types of Yukawa terms

$$\bar{\psi}_i^d \left( \hat{\phi} \begin{bmatrix} 0 \\ 1 \end{bmatrix} \right)^\dagger L\psi_j, \bar{\psi}_i \hat{\phi} \begin{bmatrix} 0 \\ 1 \end{bmatrix} R\psi_j^d, \bar{\psi}_i^u \left( \hat{\phi} \begin{bmatrix} 1 \\ 0 \end{bmatrix} \right)^\dagger L\psi_j, \bar{\psi}_i \hat{\phi} \begin{bmatrix} 1 \\ 0 \end{bmatrix} R\psi_j^u$$

are gauge invariant provided the  $\psi_i$  and  $\psi_j$  fields in the above have the same weak hypercharge. The Yukawa interaction for quarks can be written as

$$L_{YQ} = - \sum_{\text{quarks } (i,j)} \sqrt{2} \left( \bar{\psi}_i \hat{f}_{ij} \hat{\phi}^\dagger L\psi_j + \bar{\psi}_i \hat{\phi} \hat{f}_{ji}^* R\psi_j \right) \quad (20)$$

where the summation is over the three different flavors of quark fields for both  $\psi_i$  and  $\psi_j$  and

$$\hat{f}_{ij} = \begin{bmatrix} f_{ij}^u & 0 \\ 0 & f_{ij}^d \end{bmatrix}. \quad (21)$$

is a  $2 \times 2$  diagonal matrix. The Yukawa interaction for leptons does not have terms with mixed generations and is equal to

$$L_{YL} = - \sum_{\text{leptons } (i)} \sqrt{2} \left( \bar{\psi}_i \hat{f}_i \hat{\phi}^\dagger L\psi_i + \bar{\psi}_i \hat{\phi} \hat{f}_i R\psi_i \right) \quad (22)$$

where the matrix

$$\hat{f}_i = \begin{bmatrix} f_i^u & 0 \\ 0 & f_i^d \end{bmatrix} \quad (23)$$

is real and diagonal. Note that from

$$\hat{\phi} = \frac{1}{\sqrt{2}} (H + v + i\phi_a \sigma_a),$$

we get

$$L_{YL} = \sum_{\text{leptons } (i)} \bar{\psi}_i \left[ \begin{array}{c} -v\hat{f}_i - \hat{f}_i H \\ +i \left( \hat{f}_i \phi_a \sigma_a L - \phi_a \sigma_a \hat{f}_i R \right) \end{array} \right] \psi_i.$$

The gauge invariant Lagrangian for the fermion fields is

$$\begin{aligned} L_F = & \sum_{\text{quarks } (i)} \left[ \bar{\psi}_i R (i \not{D}_{q,L}) L\psi_i + \bar{\psi}_i L (i \not{D}_{q,R}) R\psi_i \right] + L_{YQ} \\ & + \sum_{\text{leptons } (i)} \left[ \bar{\psi}_i R (i \not{D}_{l,L}) L\psi_i + \bar{\psi}_i L (i \not{D}_{l,R}) R\psi_i \right] + L_{YL} \end{aligned} \quad (24)$$

which remains gauge invariant even when continued to  $n \neq 4$ . Since  $\gamma^\mu L$  is no longer equal to  $R\gamma^\mu L$  when the polarization  $\mu$  is continued to the extra-4 dimensions,  $\bar{\psi} (i \not{D}_L) L\psi$  and  $\bar{\psi} (i \not{D}_L) R\psi$  depart from  $\bar{\psi} R (i \not{D}_L) L\psi$  and  $\bar{\psi} L (i \not{D}_L) R\psi$ , and are not gauge invariant when  $n \neq 4$ . The gauge invariant 4 dimensional Lagrangian can be conveniently continued to  $n \neq 4$  without invalidating gauge symmetry by replacing  $\gamma^\mu L$  or  $R\gamma^\mu$  with  $R\gamma^\mu L$ , and replacing  $L\gamma^\mu$  or  $\gamma^\mu R$  with  $L\gamma^\mu R$ . Let us introduce the notation  $\underline{p}^\mu$  for the component of  $p^\mu$  vector in the first 4 dimensions and the notation  $p_\Delta^\mu$  for the component in the remaining dimensions. *i.e.*,

$$p^\mu = \underline{p}^\mu + p_\Delta^\mu,$$



with

$$p_\Delta^\mu = 0 \text{ if } \mu \in \{0, 1, 2, 3\}, \underline{p}^\mu = 0 \text{ if } \mu \notin \{0, 1, 2, 3\}.$$

Likewise, the Dirac matrix  $\gamma^\mu$  is decomposed as

$$\gamma^\mu = \underline{\gamma}^\mu + \gamma_\Delta^\mu$$

with  $\gamma_\Delta^\mu = 0$  when  $\mu \in \{0, 1, 2, 3\}$  and  $\underline{\gamma}^\mu = 0$  when  $\mu \notin \{0, 1, 2, 3\}$ .

The free Lagrangian derived from (24) is

$$L_F^{(0)} = \sum_{\text{leptons } (i)} \bar{\psi}_i (i \underline{\not{\partial}} - \hat{m}_i) \psi_i + \sum_{\text{quarks } (i,j)} \bar{\psi}_i (i \underline{\not{\partial}} \delta_{ij} - (\hat{m}_{ij} L + \hat{m}_{ji}^* R)) \psi_j \quad (25)$$

where

$$\underline{\not{\partial}} = \partial_\mu \underline{\gamma}^\mu = R \not{\partial} L + L \not{\partial} R$$

and the mass matrices for the fermion fields are

$$\hat{m}_i = \begin{bmatrix} m_i^u & 0 \\ 0 & m_i^d \end{bmatrix} = v \hat{f}_i \quad (26)$$

and

$$\hat{m}_{ij} = \begin{bmatrix} m_{ij}^u & 0 \\ 0 & m_{ij}^d \end{bmatrix} = v \hat{f}_{ij} \quad (27)$$

The lepton masses are  $m_i^u = v f_i^u$  and  $m_i^d = v f_i^d$  for  $\psi_i^u$  and  $\psi_i^d$  respectively.

The fermion propagator corresponding to the free Lagrangian (25) in the momentum space is

$$\frac{i}{\not{p} - m} \quad (28)$$

which is independent of  $p_\Delta$ , the component of the momentum  $p$  in the extra-4 dimensions and cannot be used for perturbative dimensional calculation. To remedy this, we add the  $CP$  invariant but gauge variant term

$$E_0 = \bar{\psi}_i \not{\partial}_\Delta \psi = \bar{\psi}_R i \not{\partial} \psi_L + \bar{\psi}_L i \not{\partial} \psi_R \quad (29)$$

to the Lagrangian of the theory. The theory so defined will have well-behaved free fermion propagator

$$\frac{i}{\not{p} - m}$$

and can be used to calculate amplitudes perturbatively under dimensional regularization scheme. But, we also incur a loss of the gauge symmetry due to  $E_0$ . Because  $E_0$  vanishes as  $n \rightarrow 4$ ,  $E_0$  does not have any tree-level contribution. At one or more loop orders, simple  $\frac{1}{n-4}$  pole factors or higher pole terms may arise from divergent loop integrals so that the contribution of  $E_0$  cannot be neglected and additional local counter terms are required to restore the gauge symmetry.

A simple and straightforward method for obtaining these finite counter terms has been proposed [15, 16] with the help of the rightmost  $\gamma_5$  scheme in which the dimension  $n$  is analytically continued after all the  $\gamma_5$  matrices have been moved to the rightmost position. For any 1-loop Feynman diagram, the amplitude calculated according to the rightmost  $\gamma_5$  scheme can be readily compared with that calculated directly from the Lagrangian under dimensional regularization with  $\gamma_5$  defined in (6). The difference between these two amplitudes can be straightforwardly calculated and is equal to the amplitude due to local counter terms that are required to restore BRST gauge symmetry.

### III. 1-LOOP ELECTROWEAK $a_\mu^{EW}$

For simplicity, we choose the Feynman gauge in which  $\alpha_B = \alpha_W = 1$  for the gauge fixing terms (14). Four diagrams are responsible for the 1-loop electroweak contribution. Those diagrams and their associated amplitudes are listed in Table I.

Adding the elements on second column in Table I amounts to a total of

$$\begin{aligned} a_\mu^{EW} [1\text{-loop}] &= \frac{Gm_\mu^2}{\pi^2} \frac{16 \left(\sin^2 \theta_W - \frac{1}{4}\right)^2 + 5}{24\sqrt{2}} \\ &= 1.948 \times 10^{-9} \end{aligned} \tag{30}$$

where we have substituted  $1.166 \times 10^{-11} \text{ Mev}^{-2}$  for the Fermi coupling constant  $G$ ,  $\sin^2 \theta_W = 1 - \frac{M_W^2}{M_Z^2} = 0.223$ , and  $105.658 \text{ MeV}$  for the muon mass  $m_\mu$  to get the numerical result.

### IV. AMPLITUDES DUE TO FINITE COUNTER TERMS AT 1-LOOP LEVEL

The finite counter term amplitude is obtained by calculating the difference arising from moving  $\gamma_5$  to the rightmost position before continuing the dimension  $n$  [16]. At 1-loop order, the diagram has to be divergent by power counting in order to have finite difference between

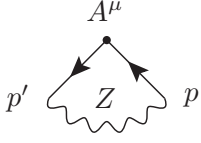
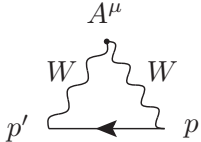
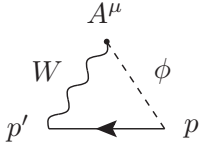
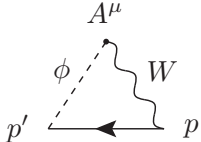
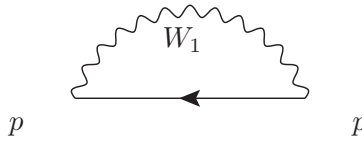
| Diagram   | Contribution to $a_\mu^{EW}$  |
|---|---|
|  | $\frac{Gm_\mu^2}{\pi^2} \frac{16(\sin^2 \theta_W - \frac{1}{4})^2 - 5}{24\sqrt{2}}$ |
|  | $\frac{Gm_\mu^2}{\pi^2} \frac{7}{24\sqrt{2}}$                                       |
|  | 0   |
|  | $\frac{Gm_\mu^2}{\pi^2} \frac{1}{8\sqrt{2}}$  |

TABLE I. 1-loop diagrams for  $a_\mu^{EW}$

different ordering of  $\gamma_5$ . Consider the 1-loop fermion self-energy correction with external muon lines and an internal  $W_1$  vector meson as shown below:



The horizontal line signifies an internal fermion line and the wavy line is a vector meson line. The Feynman amplitude for the self-energy diagram in the above is

$$\Pi_{self\mu}^{W_1} = \left(-i\frac{g_W}{2}\right)^2 \int \frac{d^n \ell}{(2\pi)^4} D(W_\mu, W_\nu; \ell) R\gamma^\mu L \frac{i}{\ell + \not{p}} R\gamma^\nu L$$

where the propagator for  $W$  meson is

$$D(W_\mu, W_\nu; \ell) = -i \frac{g_{\mu\nu}}{\ell^2 - M_W^2}.$$

Expand  $\frac{1}{\not{\ell}+i\epsilon}$  as  $\frac{1}{\not{\ell}} - \frac{1}{\not{\ell}} \not{\ell} \frac{1}{\not{\ell}} + \dots$  and note that the first order term  $\frac{1}{\not{\ell}}$  does not contribute to the integral  $\Gamma_{self}^{W_1}$  from symmetrical integration. We then have (See for Sec. IV in [16] details.)

$$\begin{aligned}\Delta\Pi_{self,\mu}^{W_1} &= i \left(\frac{g_W}{2}\right)^2 \Delta \int \frac{d^n \ell}{(2\pi)^4} D(W_\mu, W_\nu; \ell) R \gamma^\mu L \frac{1}{\not{\ell}} \not{\ell} \frac{1}{\not{\ell}} R \gamma^\nu L \\ &= i \left(\frac{g_W}{2}\right)^2 \int \frac{d^n \ell}{(2\pi)^4} \frac{D(W_\mu, W_\nu; \ell)}{(\ell^2)^2} (\gamma^\mu \not{\ell} \not{\ell} \gamma^\nu L - \gamma^\mu L \not{\ell} \not{\ell} \gamma^\nu L) \\ &= \frac{g_W^2}{8} \int \frac{d^n \ell}{(2\pi)^4} \frac{(n-4)}{(\ell^2 - M_W^2)^2} \not{\ell} L = \frac{-ig_W^2}{64\pi^2} R \not{\ell} L\end{aligned}$$

### A. Finite Counter Term Amplitude for Self-Energy

With the external fermion muon and neutrino arranged in a two component matrix  $\begin{pmatrix} \nu_\mu \\ \mu \end{pmatrix}$  field, the finite counter term contributions with internal  $W_1$ ,  $W_2$ , or  $Z$  vector meson can be similarly calculated. The combined total is

$$\Delta\Pi^{(1)} = -\frac{i}{192\pi^2} \begin{bmatrix} (g_B^2 + 3g_W^2) \not{\ell} L & 0 \\ 0 & 9(g_W^2 - g_B^2) \not{\ell} L + 16m_\mu \end{bmatrix}, \quad (31)$$

where the first and second diagonal elements correspond to neutrino  $\nu_\mu$  and muon  $\mu$ , respectively. Identify

$$\Delta Z_L = \frac{1}{64\pi^2} \begin{bmatrix} (g_B^2 + 3g_W^2) & 0 \\ 0 & 3(g_W^2 - g_B^2) \end{bmatrix},$$

and

$$\Delta Z_R = 0.$$

Then we may write

$$\Delta\Pi^{(1)} = -i(\Delta Z_L \not{\ell} L + \Delta Z_R \not{\ell} R + \Delta Z_m m_\mu).$$

The fermion propagator then becomes

$$\begin{aligned}S &= \frac{i}{\not{\ell} - m_\mu} + \frac{i}{\not{\ell} - m_\mu} \Delta\Pi^{(1)} \frac{i}{\not{\ell} - m_\mu} \\ &\simeq \left(\sqrt{Z_L} L + \sqrt{Z_R} R\right) \frac{i}{\not{\ell} - \tilde{m}} \left(\sqrt{Z_L} R + \sqrt{Z_R} L\right)\end{aligned} \quad (32)$$

where  $Z_L = 1 + \Delta Z_L$  and  $Z_R = 1 + \Delta Z_R$  and  $\tilde{m} = \left(1 + \frac{\Delta Z_L + \Delta Z_R}{2} + \Delta Z_m\right) m_\mu$ .

## B. Finite Counter Term Amplitude for Vertex

The 1-loop vertex diagram with two external fermion lines is logarithmically divergent by power counting. As a consequence, amplitude obtained with rightmost ordering of  $\gamma_5$  may differ from that obtained with the  $\gamma_5$  ordering dictated by the Lagrangian (24) by a finite amount. These finite differences for vertices with external vector  $A$ ,  $Z$ ,  $W$ , and scalar  $\phi$  are calculated and tabulated in Tables V–XI.

### 1. Extended Vertex Factor

Since an internal fermion line connects one vertex to another, the last factor  $(\sqrt{Z_L}R + \sqrt{Z_R}L)$  in (32) can be attributed to the vertex from which the fermion line leaves, the first factor  $(\sqrt{Z_L}L + \sqrt{Z_R}R)$  in (32) can be attributed to the vertex to which the fermion line flows into, and the fermion propagator stripped off these two factors effectively becomes a free propagator  $\frac{i}{\not{p}-\tilde{m}}$ . For an external incoming or outgoing fermion line,  $(\sqrt{Z_L}R + \sqrt{Z_R}L)$  or  $(\sqrt{Z_L}L + \sqrt{Z_R}R)$  can be absorbed into the wavefunction renormalization of the external spinor. i.e., the fermion propagator can be regarded as  $\frac{i}{\not{p}-\tilde{m}}$  provided we multiply the vertex factor on the left by  $(\sqrt{Z_L}R + \sqrt{Z_R}L)$  and on the right by  $(\sqrt{Z_L}L + \sqrt{Z_R}R)$ . Diagrammatically, we shall use a large black dot to denote such an "extended" vertex that includes contributions from all finite counter terms and the wavefunction normalization factors  $(\sqrt{Z_L}R + \sqrt{Z_R}L)$  on the left and  $(\sqrt{Z_L}L + \sqrt{Z_R}R)$  on the right. The 1-loop vertex factors for all possible black dots are calculated and listed in Tables II and III.

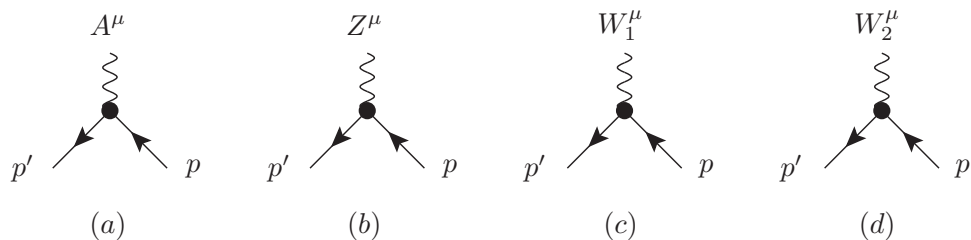


FIG. 1. Extended Vertex Diagrams for fermion-vector-fermion

| Figure | $\Gamma^\mu - \Gamma_{tree}^\mu$  |
|--------|---|
| 1(a)   | $-ie \frac{g_W^2}{32\pi^2} \begin{bmatrix} 1 & 0 \\ 0 & -1 \end{bmatrix} \gamma^\mu L$  |
| 1(b)   | $\frac{i\sqrt{g_W^2+g_B^2}}{128\pi^2} \left( \frac{3g_W^4+g_B^4}{g_W^2+g_B^2} \begin{bmatrix} 1 & 0 \\ 0 & -1 \end{bmatrix} \gamma^\mu L + g_B^2 \begin{bmatrix} 0 & 0 \\ 0 & 8\gamma^\mu - 12\gamma^\mu L \end{bmatrix} \right)$ |
| 1(c)   | $\frac{3ig_W(g_W^2+g_B^2)}{128\pi^2} \begin{bmatrix} 0 & 1 \\ 1 & 0 \end{bmatrix} \gamma^\mu L$   |
| 1(d)   | $\frac{3ig_W(g_W^2+g_B^2)}{128\pi^2} \begin{bmatrix} 0 & -i \\ i & 0 \end{bmatrix} \gamma^\mu L$  |

TABLE II. Extended Vertex Factors for fermion-vector-fermion at 1-loop order

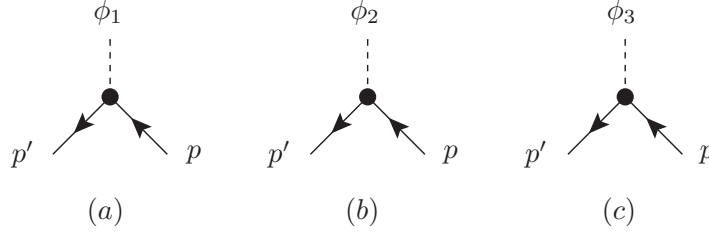


FIG. 2. Extended Vertex Diagrams for fermion-scalar-fermion

## V. FINITE-COUNTER-TERM CONTRIBUTION TO $a_\mu^{EW}$

To obtain the finite-counter-term contribution for  $a_\mu^{EW}$ , replace the fermion vertex factors in each of the four diagram of Table I with the large black dot representing the extended vertex as shown in Table IV. The amplitude with  $a_\mu^{EW}$  [tree] and  $a_\mu^{EW}$  [1-loop] subtracted out is the finite-counter-term to  $a_\mu^{EW}$ .

$a_\mu^{EW}$  [Finite Counter term] is obtained by summing over the second column. The result is

$$-\frac{\alpha G m_\mu^2}{384\sqrt{2}\pi^3} \csc^2(2\theta_W) (6 \cos(6\theta_W) - 8 \cos(4\theta_W) + 109 \cos(2\theta_W) - 37)$$

which is numerically evaluated to

$$a_\mu^{EW} [\text{Finite Counter term}] = -1.67541 \times 10^{-12} \quad (33)$$

| Figure | $\Gamma - \Gamma_{tree}$  |
|--------|---|
| 2(a)   | $f \frac{(g_W^2 - 14g_B^2)}{128\pi^2} \begin{bmatrix} 0 & R \\ -L & 0 \end{bmatrix}$      |
| 2(b)   | $-if \frac{(g_W^2 - 14g_B^2)}{128\pi^2} \begin{bmatrix} 0 & R \\ L & 0 \end{bmatrix}$     |
| 2(c)   | $f \frac{(g_W^2 - 43g_B^2)}{128\pi^2} \begin{bmatrix} 0 & 0 \\ 0 & (L - R) \end{bmatrix}$ |

TABLE III. Extended Vertex Factors for fermion-scalar-fermion

| Diagram | Finite-counter-term Contribution to $a_\mu^{EW}$  |
|---------|---|
|         | $\frac{\alpha G m_\mu^2}{12\sqrt{2}\pi^3} \csc^2(2\theta_W) \times (6 \sin^6(\theta_W) - 7 \sin^4(\theta_W) + 11 \sin^2(\theta_W^2) + 4)$ |
|         | $-\frac{7\alpha G m_\mu^2}{17\sqrt{2}\pi^3} \csc^2(2\theta_W)$  |
|         | $\frac{5\alpha G m_\mu^2}{128\sqrt{2}\pi^3} \csc^2(2\theta_W) (3 \cos(2\theta_W) - 5)$  |
|         | 0   |

TABLE IV. Finite-counter-term Diagrams

where we have set  $\alpha = \frac{1}{137.036}$ .

## VI. CONCLUSION

In the dimensional regularization scheme, simply removing the pole terms from the amplitudes of 1-loop diagrams does not yield renormalized amplitudes that satisfy the BRST

gauge symmetry. Instead, some finite renormalization terms have to be added. The renormalized amplitudes for all 1-loop diagrams calculated in the straightforward dimensional regularization scheme with finite counter term renormalization are equal to those obtained in the rightmost  $\gamma_5$  scheme. This means we can be spared the tedious finite renormalization procedures if the rightmost  $\gamma_5$  scheme is adopted as we have shown in this paper for the evaluation of  $a_\mu = \frac{g_\mu - 2}{2}$ , where  $g_\mu$  is the muon gyromagnetic ratio.

The  $a_\mu^{EW}$  [Finite Counter term] =  $-1.67541 \times 10^{-12}$  we have arrived at in (33) due to the finite counter terms arising from electroweak interaction in the standard model is only about one-thousandth of the  $a_\mu^{EW}$  [1-loop] =  $1.948 \times 10^{-9}$  in (30) or the difference  $\Delta a_\mu = 2.81 \times 10^{-9}$  between experiment and theory in (5). The finite counter term contribution to the muon magnetic moment is therefore not significant enough to account for the discrepancy between experiment and theoretical prediction by standard model.

## Appendices

### Appendix A: Counter term Amplitudes due to Vertex Diagrams

Vertex diagrams that are relevant to the calculation of the finite counter terms contributing to the muon anomalous magnetic moment are drawn below in Figures 3–9 with corresponding amplitudes listed in Tables V–XI.

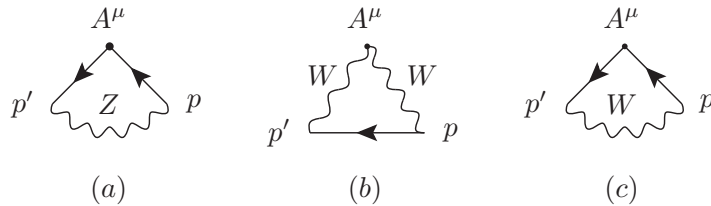


FIG. 3. Vertex Diagrams for  $\bar{\Psi} A^\mu \Psi$



| Figure | $\Delta\Gamma^{A^\mu}$  |
|--------|---|
| 3(a)   | $\frac{ie(g_W^2-3g_B^2)}{64\pi^2}\gamma^\mu \begin{bmatrix} 0 & 0 \\ 0 & 1 \end{bmatrix} L$ |
| 3(b)   | $\frac{-ieg_W^2}{16\pi^2}\gamma^\mu \begin{bmatrix} 1 & 0 \\ 0 & -1 \end{bmatrix} L$        |
| 3(c)   | $\frac{ieg_W^2}{32\pi^2}\gamma^\mu \begin{bmatrix} 1 & 0 \\ 0 & 0 \end{bmatrix} L$          |

TABLE V. Counter term Amplitude for fermion- $A^\mu$ -fermion vertex

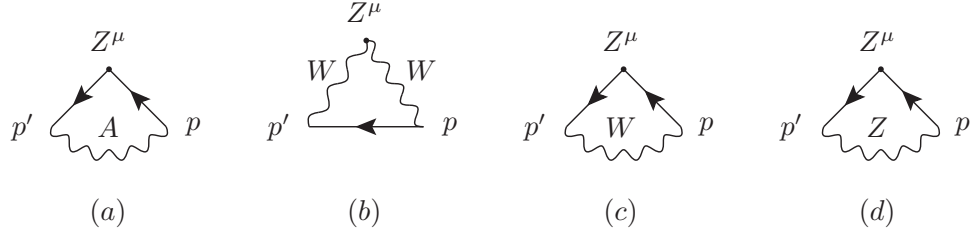


FIG. 4. Vertex Diagrams for  $\bar{\Psi}Z^\mu\Psi$

| Figure | $\Delta\Gamma^{Z^\mu}$   |
|--------|--|
| 4(a)   | $\frac{ie^2\sqrt{g_B^2+g_W^2}}{16\pi^2}\gamma^\mu \begin{bmatrix} 0 & 0 \\ 0 & R-L \end{bmatrix}$  |
| 4(b)   | $\frac{ieg_W^3}{16\pi^2}\gamma^\mu \begin{bmatrix} 1 & 0 \\ 0 & -1 \end{bmatrix} L$  |
| 4(c)   | $\frac{ig_W^2}{32\pi^2\sqrt{g_B^2+g_W^2}}\gamma^\mu \begin{bmatrix} -g_W^2 & 0 \\ 0 & (g_W^2+g_B^2) \end{bmatrix} L$   |
| 4(d)   | $\frac{i(g_B^2+g_W^2)^{\frac{3}{2}}}{64\pi^2}\gamma^\mu \begin{bmatrix} L & 0 \\ 0 & \frac{4g_B^4-(g_W^4-3g_B^2g_W^2+8g_B^4)L}{(g_B^2+g_W^2)^2} \end{bmatrix}$ |

TABLE VI. Counter term Amplitude for fermion- $Z^\mu$ -fermion vertex

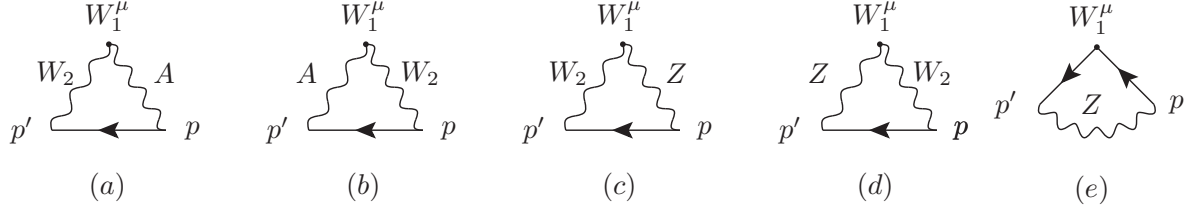


FIG. 5. Vertex Diagrams for  $\bar{\Psi}W_1^\mu\Psi$

| Figure | $\Delta\Gamma^{W_1^\mu}$  |
|--------|---|
| 5(a)   | $\frac{3ie^2g_W}{32\pi^2}\gamma^\mu \begin{bmatrix} 0 & 1 \\ 0 & 0 \end{bmatrix} L$                               |
| 5(b)   | $\frac{3ie^2g_W}{32\pi^2}\gamma^\mu \begin{bmatrix} 0 & 0 \\ 1 & 0 \end{bmatrix} L$                               |
| 5(c)   | $\frac{ie^2g_W}{64\pi^2g_B}\gamma^\mu \begin{bmatrix} 0 & 2g_W^2 - g_B^2 \\ 2(g_W^2 + g_B^2) & 0 \end{bmatrix} L$ |
| 5(d)   | $\frac{ie^2g_W}{64\pi^2g_B}\gamma^\mu \begin{bmatrix} 0 & 2(g_W^2 + g_B^2) \\ 2g_W^2 - g_B^2 & 0 \end{bmatrix}$   |
| 5(e)   | $\frac{-ig_W(g_W^2 - g_B^2)}{64\pi^2}\gamma^\mu \begin{bmatrix} 0 & 1 \\ 1 & 0 \end{bmatrix} L$                   |

TABLE VII. Counter term Amplitude for fermion- $W_1^\mu$ -fermion vertex

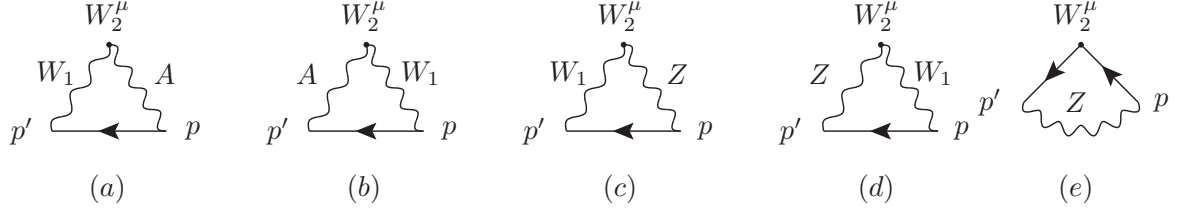


FIG. 6. Vertex Diagrams for  $\bar{\Psi}W_2^\mu\Psi$

| Figure | $\Delta\Gamma^{W_2^\mu}$  |
|--------|---|
| 6(a)   | $\frac{3ie^2g_W}{32\pi^2}\gamma^\mu \begin{bmatrix} 0 & -i \\ 0 & 0 \end{bmatrix} L$                              |
| 6(b)   | $\frac{3ie^2g_W}{32\pi^2}\gamma^\mu \begin{bmatrix} 0 & 0 \\ i & 0 \end{bmatrix} L$                               |
| 6(c)   | $\frac{e^2g_W}{64\pi^2g_B}\gamma^\mu \begin{bmatrix} 0 & 2g_W^2 - g_B^2 \\ -2(g_W^2 + g_B^2) & 0 \end{bmatrix} L$ |
| 6(d)   | $\frac{e^2g_W}{64\pi^2g_B}\gamma^\mu \begin{bmatrix} 0 & 2(g_W^2 + g_B^2) \\ -2g_W^2 + g_B^2 & 0 \end{bmatrix} L$ |
| 6(e)   | $\frac{-ig_W(g_W^2 - g_B^2)}{64\pi^2}\gamma^\mu \begin{bmatrix} 0 & -i \\ i & 0 \end{bmatrix} L$                  |

TABLE VIII. Counter term Amplitude for fermion- $W_2^\mu$ -fermion vertex

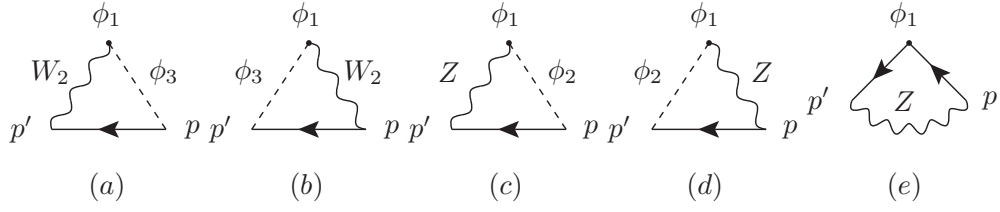


FIG. 7. Vertex Diagrams for  $\bar{\Psi}\phi_1\Psi$

| Figure | $\Delta\Gamma^{\phi_1}$   |
|--------|---|
| 7(a)   | $\frac{fg_W^2}{128\pi^2} \begin{bmatrix} 0 & -R \\ 0 & 0 \end{bmatrix}$           |
| 7(b)   | $\frac{fg_W^2}{128\pi^2} \begin{bmatrix} 0 & 0 \\ L & 0 \end{bmatrix}$            |
| 7(c)   | $\frac{f(g_W^2 - g_B^2)}{128\pi^2} \begin{bmatrix} 0 & -R \\ 0 & 0 \end{bmatrix}$ |
| 7(d)   | $\frac{f(g_W^2 - g_B^2)}{128\pi^2} \begin{bmatrix} 0 & 0 \\ L & 0 \end{bmatrix}$  |
| 7(e)   | $\frac{fg_B^2}{8\pi^2} \begin{bmatrix} 0 & -R \\ L & 0 \end{bmatrix}$             |

TABLE IX. Counter term Amplitude for fermion- $\phi_1$ -fermion vertex

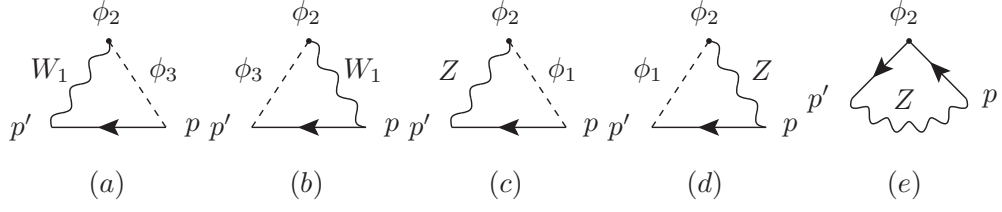


FIG. 8. Vertex Diagrams for  $\bar{\Psi}\phi_2\Psi$

| Figure | $\Delta\Gamma^{\phi_2}$   |
|--------|---|
| 8(a)   | $\frac{ifg_W^2}{128\pi^2} \begin{bmatrix} 0 & R \\ 0 & 0 \end{bmatrix}$         |
| 8(b)   | $\frac{ifg_W^2}{128\pi^2} \begin{bmatrix} 0 & 0 \\ L & 0 \end{bmatrix}$         |
| 8(c)   | $\frac{if(g_W^2-g_B^2)}{128\pi^2} \begin{bmatrix} 0 & R \\ 0 & 0 \end{bmatrix}$ |
| 8(d)   | $\frac{if(g_W^2-g_B^2)}{128\pi^2} \begin{bmatrix} 0 & 0 \\ L & 0 \end{bmatrix}$ |
| 8(e)   | $\frac{ifg_B^2}{8\pi^2} \begin{bmatrix} 0 & R \\ L & 0 \end{bmatrix}$           |

TABLE X. Counter term Amplitude for fermion- $\phi_2$ -fermion vertex

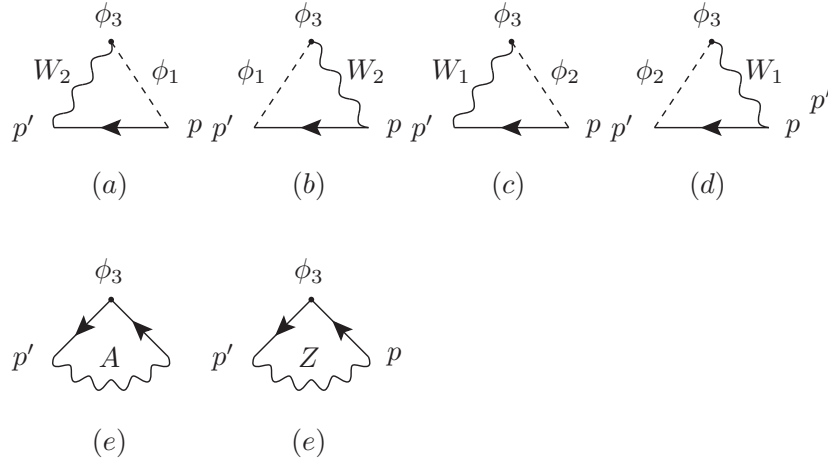


FIG. 9. Vertex Diagrams for  $\bar{\Psi}\phi_3\Psi$

| Figure | $\Delta\Gamma^{\phi_3}$  |
|--------|--|
| 9(a)   | $\frac{fg_W^2}{128\pi^2} \begin{bmatrix} 0 & 0 \\ 0 & R \end{bmatrix}$                                       |
| 9(b)   | $\frac{fg_W^2}{128\pi^2} \begin{bmatrix} 0 & 0 \\ 0 & -L \end{bmatrix}$                                      |
| 9(c)   | $\frac{fg_W^2}{128\pi^2} \begin{bmatrix} 0 & 0 \\ 0 & R \end{bmatrix}$                                       |
| 9(d)   | $\frac{fg_W^2}{128\pi^2} \begin{bmatrix} 0 & 0 \\ 0 & -L \end{bmatrix}$                                      |
| 9(e)   | $\frac{e^2 f}{2\pi^2} \begin{bmatrix} 0 & 0 \\ 0 & R - L \end{bmatrix}$                                      |
| 9(f)   | $\frac{e^2 f}{16\pi^2} \left(3 - 5\frac{g_B^2}{g_W}\right) \begin{bmatrix} 0 & 0 \\ 0 & R - L \end{bmatrix}$ |

TABLE XI. Counter term Amplitude for fermion- $\phi_3$ -fermion vertex

- 
- [1] G.W. Bennett et al., Phys. Rev. D73, 072003 (2006).
- [2] P.J. Mohr, B.N. Taylor, and D.B. Newell, CODATA Group, Rev. Mod. Phys. 84, 1527 (2012).
- [3] For example, see Problem 7.2 in A Modern Introduction to Quantum Field Theory by Michele Maggiore.
- [4] T. Aoyama et al., Phys. Rev. Lett. 109, 111808 (2012); T. Aoyama et al., Phys. Rev. Lett. 109, 111807 (2012); T. Kinoshita and M. Nio, Phys. Rev. D73, 013003 (2006); T. Aoyama et al., Phys. Rev. Lett. 99, 110406 (2007); T. Kinoshita and M. Nio, Phys. Rev. D70, 113001 (2004); T. Kinoshita, Nucl. Phys. B144, 206 (2005)(Proc. Supp.); T. Kinoshita and M. Nio, Phys. Rev. D73, 053007 (2006); A.L. Kataev, arXiv:hep-ph/0602098 (2006); M. Passera, J. Phys. G31, 75 (2005).
- [5] R. Jackiw and S. Weinberg, Phys. Rev. D5, 2396 (1972); G. Altarelli et al., Phys. Lett. B40, 415 (1972); I. Bars and M. Yoshimura, Phys. Rev. D6, 374 (1972); K. Fujikawa, B.W. Lee, and A.I. Sanda, Phys. Rev. D6, 2923 (1972).
- [6] C. Gnendiger, D. Stockinger, H. Stockinger-Kim, Phys. Rev. D88, 053005 (2013); A. Czarnecki et al., Phys. Rev. D67, 073006 (2003), Erratum ibid. Phys. Rev. D73, 119901 (2006); S. Heinemeyer, D. Stockinger, and G. Weiglein, Nucl. Phys. B699, 103 (2004); T. Gribouk and A. Czarnecki, Phys. Rev. D72, 053016 (2005); A. Czarnecki, B. Krause, and W.J. Marciano, Phys. Rev. Lett. 76, 3267 (1996); A. Czarnecki, B. Krause, and W.J. Marciano, Phys. Rev. D52, 2619, (1995); S. Peris, M. Perrottet, and E. de Rafael, Phys. Lett. B355, 523 (1995); T. Kukhto et al, Nucl. Phys. B371, 567 (1992).
- [7] C. Bouchiat and L. Michel, J. Phys. Radium 22, 121 (1961); M. Gourdin and E. de Rafael, Nucl. Phys. B10, 667 (1969); S.J. Brodsky and E. de Rafael, Phys. Rev. 168, 1620 (1968).
- [8] M. Davier et al., Eur. Phys. J. C71, 1515 (2011).
- [9] arXiv:0901.0306 [hep-ph] (2009).
- [10] G. 't Hooft and M. Veltman, Nucl. Phys. **B44**, 189 (1972).
- [11] P. Breitenlohner and D. Maison, Commun. math. Phys. **52**, 11 (1977).
- [12] D. Sanchez-Ruiz, Phys. Rev. **D68**, 025009 (2003); C. P. Martin and D. Sanchez-Ruiz, Nucl. Phys. **B572**, 387 (2000).; R. Ferrari and P. A. Grassi, Phys. Rev. **D60**, 065010 (1999); R. Ferrari, A. Le Yaouanc, L. Oliver, and J. C. Raynal, Phys. Rev. **D52**, 3036 (1995); Guy



- Bonneau, Nucl. Phys. **B177**, 523 (1981).
- [13] C. Becchi, A. Rouet and R. Stora, Phys. Lett. **B52**, 344 (1974); Comm. Math. Phys. **42**, 127 (1975); Ann. of Phys. **98**, 287 (1976). I.V. Tyutin, Lebedev Institute preprint 39 (1975).
- [14] H. Cheng and E. C. Tsai, Phys. Lett. **B176**, 130 (1986); Phys. Rev. **D40**, 1246 (1989).
- [15] E. C. Tsai, Phys. Rev. **D83**, 025020 (2011).
- [16] E. C. Tsai, Phys. Rev. **D83**, 065011 (2011).